Full Paper

Propellants, Explosives, Pyrotechnics

DOI: 10.1002/prep.201700230

Fragmentation of Ammonium Nitrate Particles under Thermal Cycling

Filippo Maggi*[a] and Priya Garg[b]

Abstract: Ammonium nitrate finds application in explosives and chlorine-free slow-burning propellants. Different phases are known for this ammonium salt, each of them featured by peculiar bulk densities. As a consequence, the variation of storage temperature induces processes of expansion-contraction in the crystals, unless specific stabilization is performed. In this paper, a batch of raw ammonium nitrate particles has been thermally cycled between −30 °C to +60 °C and analyzed. Microscopic observations, particle size measurement, and X-ray microtomography showed that the particles undergo a progressive fragmentation process, with opening of internal cracks and voids. The tested material halved its mass-mean diameter after five thermal cycles. As a term of comparison, a phase-stabilized ammonium nitrate batch was tested under the same conditions, showing no effect.

Keywords: ammonium nitrate · phase transition · fragmentation · thermal cycling

1 Introduction

The ammonium nitrate (AN) is one of the more interesting ammonium salts from the commercial viewpoint. It finds extensive application in the field of nitrogen-based fertilizers and energetic materials [1]. In the World War II the salt was used as ingredient in high explosives. Currently, AN can be found in conjunction with fuels, mixed with other explosives, or in emulsions (e.g. ammonal, amatol, ANFO) [2]. In modern solid propellants, the use of ammonium nitrate is restricted to slow-burning compositions and has the advantage of gaseous and chlorine-free combustion products. This aspect enables the use of the oxidizer in eco-friendly propellants, non-corrosive gas-generators, automotive airbags, and low-signature propellants (minimizing the secondary smoke). High hygroscopicity and presence of multiple phases, having different densities, represent two out of the most important issues preventing its application.

The knowledge, control, or suppression of phase transitions are fundamental for AN industrial application. For example, propellants with nonstabilized AN have been reported to crack after thermal cycles involving crystal transformations [3]. At author's knowledge, seven crystalline structures are acknowledged, six of them occurring at ambient pressure. A seventh one is observed at elevated pressures. Each of them is associated to a specific lattice arrangement and to a different bulk density. A complete discussion about both stable and metastable states was published by Nagatani and co-authors [4]. From a practical application, the transformation between the phase IV and III is of paramount interest and is referred to occur at 32 °C. As reported by Griffith, such process is moisture sensitive, and the suppression of phase III is observed for dry conditions [5]. In its place, a metastable transition IV–II is obtained. The temperature for such event can be slightly inhomogeneous across different authors. Nagatani and co-authors report the occurrence at 51 °C while for Engel and Menke the transition is at 55 °C. Table 1 reports a compact summary about the most interesting structure evolutions of pure AN at ambient pressure, adapted from [6].

Table 1. Phase transitions of ammonium nitrate. Adapted from [6].

Phase	V	IV	III	II	I
	Tetragonal	Orthorhombic	Orthorhombic	Tetragonal	Cubic
Stability °C Humid	< −18	−18 to 32	32 to 84	84 to 125	125 to melt
Stability °C Dry	< −18	−18 to 55	suppressed	55 to 125	125 to melt

[a] *F. Maggi*
Dept. Aerospace Science and Technology
Politecnico di Milano
Via La Masa 34, 20156 Milan, Italy
**e-mail: filippo.maggi@polimi.it*
[b] *P. Garg*
Dept. Aerospace Science and Technology
Politecnico di Milano
Via La Masa 34, 20156 Milan, Italy

The introduction of potassium ions in the crystal lattice by co-crystallization or melting demonstrated good efficacy as stabilizing methodology. Among the options, potassium nitrate revealed a remarkable property of lowering the transition temperature, reducing the volume change and the sensitivity to moisture [7]. Campbell and Campbell noted that a minimum fraction of additive is required to obtain a complete stabilization at temperatures relevant to storage conditions [8].

The present paper investigates the behaviour of non-stabilized ammonium nitrate under thermal cycles. The crystals are thermally cycled under dry conditions. The evolution of their physical properties is progressively monitored showing particle size alterations, morphology, and X-ray microtomography. Comparison with a phase-stabilized ammonium nitrate based on potassium nitrate is reported.

2 Experimental

2.1 Materials

Two types of ammonium nitrate have been considered in this study. One is non-stabilized AN and one is phase stabilized AN of similar granulometry.

The nonstabilized ammonium nitrate (labeled as "Raw AN") has been produced by Yara (Lot 14962-1-2). The product contains Lilamin, a C16-18-alkyl-amine anticaking agent in a mass fraction lower than 0.15%. The nominal particle size mentioned by the supplier is 326 μm.

The phase-stabilized ammonium nitrate (PSAN) powder is labeled "PSAN-Coarse" and has been supplied within the frame of the GRAIL project by the Fraunhofer Institute for Chemical Technology, Karlsruhe, Germany (ICT). The product was stabilized by adding 7 wt.% of potassium nitrate, obtaining a suppression of the IV to III phase transition, as documented in the literature [8]. The anticaking agent AEROSIL 200 was added in the amount of 0.5 wt.%. The nominal particle size was 155.7 μm (sieves).

Laser diffraction of the virgin powders has been conducted through Malvern Mastersizer 2000, using Scirocco dry dispersion system. For all the materials, a monomodal behavior was evidenced. The Raw-AN showed a quite narrow distribution featuring a span of 1.18. and a diameter for the 50th volume percentile d(0.5) = 363 μm. The PSAN-Coarse had a d(0.5) = 165 μm, with a span of 2.21. Details of the particle size analysis are given in Table 2 where the reader can find also the values for the mass-mean diameter $D_{4,3}$, the surface-mean diameter $D_{3,2}$, and the data for 10th, 50th and 90th volume percentiles.

Table 2. Particle size analysis of original materials through laser diffraction

Material	d(0.1) (μm)	d(0.5) (μm)	d(0.9) (μm)	$D_{3,2}$ (μm)	$D_{4,3}$ (μm)	Span
Raw AN	188	363	618	286	384	1.18
PSAN Coarse	49.8	165	415	96.2	204	2.21

2.2 Techniques

The two powders were placed in polypropylene jars, then enclosed in a sealed glass vessel containing silica gel dessicant salts. The powder transfer to the jars was performed inside a bag box filled with Argon. The samples were then thermally cycled between −30 °C to +60 °C. This cycling was performed manually by moving the vessel between an oven fixed at +60 °C and a refrigeration system at −30 °C. Each status was maintained for 24 hours. The samples were kept at room temperature (around 25 °C) for 1 hour when switching between the two conditions. A total of 5 thermal cycles was performed.

Particle modification was initially observed by monitoring the variation of two of the main morphology parameters: in this specific case, size and shape [9]. Few hundreds of milligrams were sampled after the first, the third, and the fifth thermal cycle. Laser diffraction analysis was performed using Malvern Mastersizer 2000, equipped with Scirocco dry dispersion system. A Standard Operating Procedure (SOP) was created for each type of oxidizer at the beginning of the campaign. The air pressure rate was fixed to 0.2 MPa for all the three samples and the tray vibration feed rate was set to 90% for Raw-AN whereas for PSAN Coarse it was kept to 50% to ensure proper laser obscuration. These analysis conditions ensured absence of clustering and minimization of crystal jet-milling for the virgin materials by the dry dispersion methodology. The particle size distribution of the oxidizers has been reported by taking average of 5 runs, computed by Malvern Mastersizer 2000 software (version 5.61). The particle shape was qualitatively analyzed through digital imaging from a standard optical desktop microscope.

Further analyses have been conducted on the microstructure of the Raw-AN material. The internal modification of the crystal between initial condition and end of the thermal cycling was visualized through an NSI X-25 Digital X-Ray micro computed tomography system. The specific settings chosen for the analysis ensured a pixel pitch of 5.5 μm.

3 Results

3.1 Particle Size

The particle size distribution detected through laser granulometry across the thermal cycling is reported in Figure 1 for Raw-AN and Figure 2 for PSAN-Coarse.

The powder Raw-AN is undergoing a process of fragmentation. The monomodal nature is maintained but the peak of the curve shifts progressively towards finer values

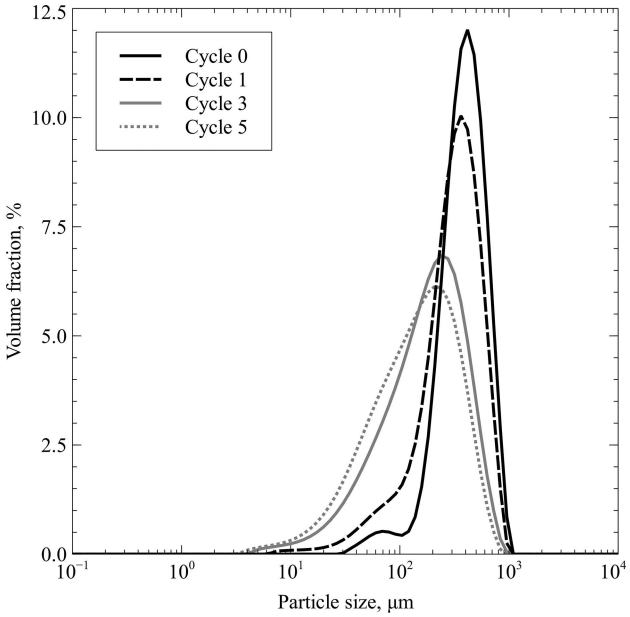

Figure 1. Particle size distribution curves for Raw-AN sample after different cycles

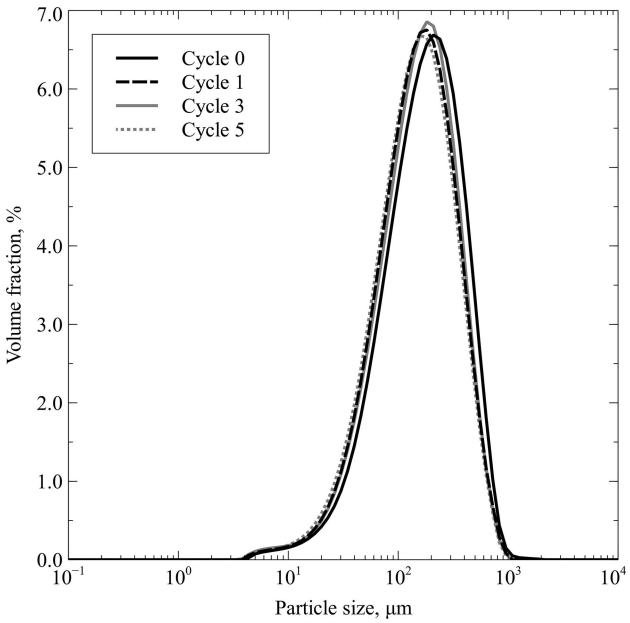

Figure 2. Particle size distribution curves for PSAN-Coarse sample after different cycles

and the amplitude of the distribution increments. The distribution loses part of the coarsest component while the fraction finer than 100 μm is incremented.

The numerical data for the analysis of Raw-AN are reported in Table 3. A substantial decrement of all dimensional parameters can be observed, confirming a progressive fragmentation of the samples. On the other hand,

Table 3. Particle size characterization data for Raw-AN sample after different cycles

Cycle	d(0.1) (μm)	d(0.5) (μm)	d(0.9) (μm)	$D_{3,2}$ (μm)	$D_{4,3}$ (μm)	Span
0	188	363	618	286	384	1.18
1	101	298	552	175	316	1.51
3	42.2	171	414	86.4	204	2.17
5	32.9	137	364	68.7	172	2.41

the increment of the span documents the broadening of the distribution. The size reduction is more evident between cycle 1 and cycle 3, rather than between cycle 3 and 5. The process seems to approach a plateau behavior. The reciprocal variations in d(0.1) and d(0.9) parameters suggest that the size reduction is not uniform, with consequent accumulation of the fine fraction. The same indication can be obtained when comparing the variation of $D_{4,3}$ and $D_{3,2}$, being the former more sensitive to the presence of coarse particles.

The particle size distribution of the PSAN-Coarse lot is reported in Figure 2. Here, curves show a minor decrement of the peak size after the first thermal cycle. The size is then stabilized and does not change throughout the rest of the cycles.

The numerical data representing the distributions of PSAN-Coarse powders are reported in Table 4. The variation of d(0.1) throughout the thermal cycles is minimal and does not reveal a substantial increment in the fine component of the distribution. A small reduction of the d(0.9) is mainly concentrated between cycle 0 and cycle 1 and indicates a minor decrement of the coarsest component of the distribution. A comparison with the results obtained for Raw-AN (Table 3) suggests that the dimensional variation of the phase-stabilized AN is almost negligible.

Table 4. Particle size characterization data for PSAN-Coarse sample after different cycles

Cycle	d(0.1) (μm)	d(0.5) (μm)	d(0.9) (μm)	$D_{3,2}$ (μm)	$D_{4,3}$ (μm)	Span
0	49.8	165	415	96.2	204	2.21
1	43.9	142	363	84.9	178	2.24
3	44.4	147	366	84.9	181	2.18
5	41.5	136	352	80.9	172	2.28

3.2 Particle Shape

The modification of the particle shapes induced by the fragmentation due to the thermal cycling was observed for both Raw-AN and PSAN-Coarse powders. Two images have been taken for each lot with a magnification of 5×. Un-

cycled powders are reported respectively in Figure 3a and Figure 4a. Imaging of particles after five thermal cycles are reported respectively in Figure 3b and Figure 4b. The reader should be warned that particles are not the same ones but are randomly sampled.

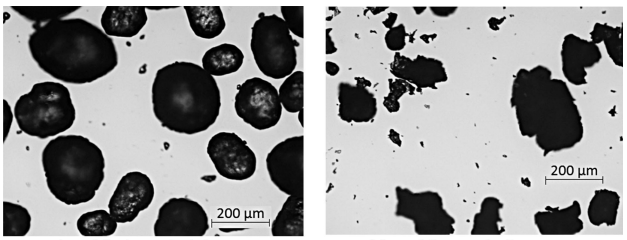

Figure 3. Raw-AN particles viewed under microscope (magnification: 5 ×)

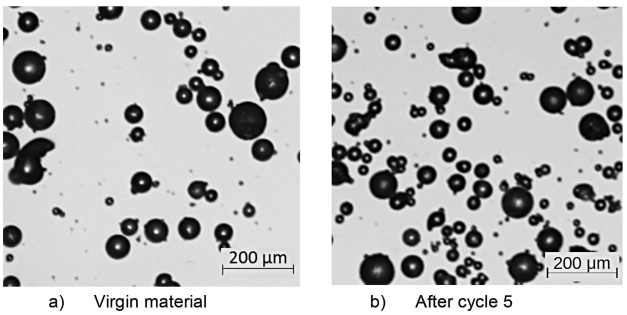

Figure 4. PSAN-Coarse particles viewed under microscope (magnification: 5 ×)

The original material of Raw-AN lot (Figure 3a) features rounded, nearly spherical shapes. Despite the superficial texture was not investigated, the edges visible from the microscopic top view appear smooth. After the thermal cycles (Figure 3b), the material contains fragments of varying size. Particle edges are irregular in shape. The rounded aspect is lost. This observation confirms the fragmentation process already evidenced in laser diffraction analysis.

The original PSAN-Coarse sample (Figure 4a) is a prilled material. The particles look like regular spheres of varying size. After 5 thermal cycles (Figure 4b) the particle quality seems to be unchanged. The surface is still smooth and the shape is spherical, as the original particles. Also in this case, the images confirm the result obtained from the laser diffraction analysis, where fragmentation was not detected.

3.3 Microstructure

An X-ray computed microtomography analysis was conducted on Raw-AN particles to investigate the source of the fragmentation attitude.

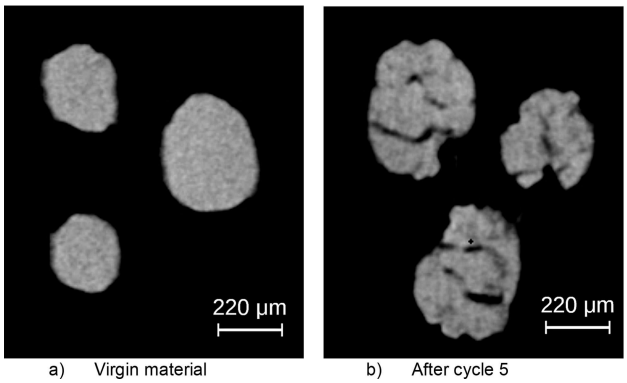

Figure 5. Tomographic slices of Raw-AN particles before and after five thermal cycles (Pixel pitch −5.5 µm/pixel)

Few coarse particles with similar size have been extracted from both virgin material and fully cycled sample. The powders have been mounted on a sticky holder and were imaged in the same scanning session to ensure the uniform exposure and post-processing. Examples of slices extracted from three-dimensional reconstructions have been reported in Figure 5a for the virgin material and Figure 5b for particles after five thermal cycles.

The tomographic slice of Raw-AN material at the initial condition (Figure 5a) shows a compact internal microstructure. Also from this view, the particle edges appear smooth and regular. The internal microstructure of the cycled powder (Figure 5b) is not compact. Cracks open across the particles, generating internal voids. The edges are not regular, suggesting that some fragments may have detached, following the internal cracking. It is important to underline that the visualized powder belongs to the group of those particles that did not fragment during the process and is representative of the coarse part of the distribution observed in Figure 1 and Table 3 for cycle 5 condition.

4 Discussion

The process of phase transition in ammonium nitrate powders appears to be critical for the health of the single crystals. According to the temperature ranges of the stable and metastable structures, the crystal was cycled between phases II and V. Few iterations were enough to fragment the non-stabilized powders. The damage was progressive and mainly affected the coarsest fraction of the distributions. Microscopic images showed that the particles lose fragments of irregular shape from the sides or cracked into smaller pieces. Laser diffraction measurement showed a progressive decrement of the main size parameters. The PSAN prills, using potassium nitrate stabilization, were characterized by a rounded shape. These particles did not show important fragmentation effects and were almost insensitive to ther-

mal processing. Both particle size measurements and microscopic views supported these considerations.

The microtomography analysis showed that the attitude of particle fragmentation, observed in the nonstabilized Raw-AN, derived from the internal damage that accumulated inside the crystals during cycles. Tomographic slices of randomly chosen coarse particles showed the presence of cracks and vacuoles inside the bulk. If compared to the original state, the cycled items may be weaker and prone to partial fragmentation or crystal cleavage in case of further thermal and mechanical processing.

5 Conclusion

Fragmentation attitude of ammonium nitrate nonstabilized particles was investigated in the paper. The process was analyzed through laser granulometry, optical microscopy, and tomography suggesting a degradation of the crystal with progressive fragmentation into finer pieces of irregular shape. X-ray analyses were used to highlight the accumulation of damages inside particles.

Parallel analyses were also performed on a sample of PSAN, showing no significant sensitivity to thermal cycling and demonstrating that, in this respect, the stabilization based on potassium nitrate is effective in maintaining the crystal quality, even after some thermal cycles.

Acknowledgements

The paper was partially supported by the GRAIL project, a European Union's Horizon 2020 research and innovation program under grant agreement no. 638719. The work was part of a cooperative action between the AMALA (Advanced Manufacturing Laboratory) and SPLab (Space Propulsion Laboratory) of Politecnico di Milano.

References

[1] C. Oommen, S. R. Jain, Ammonium nitrate: a promising rocket propellant oxidizer, *J. Hazard. Mater.* **1999**, A67, 253–281.
[2] S. Chaturvedi, P. N. Dave, Review on Thermal Decomposition of Ammonium Nitrate, *J. Energ. Mater.* **2013**, *31*, 1–26.
[3] P. Carvalheira, G. M. H. J. L. Gadiot, W. P. C. de Klerk, Thermal decomposition of phase-stabilised ammonium nitrate (PSAN), hydroxyl-terminated polybutadiene (HTPB) based propellants. The effect of iron (III) oxide burning-rate catalyst, *Thermochim. Acta* **1995**, *269*, 273–293.
[4] M. Nagatani, S. Tetsuro, S. Minoru, S. Hiroshi, S. Syûzô, Heat capacities and thermodynamic properties of ammonium nitrate crystal: phase transitions between stable and metastable phases, *Bull. Chem. Soc. Jpn.* **1967**, *40,* 1833–1844.
[5] E. J. Griffith, Phase transition of the ammonium nitrate-magnesium nitrate system, *J. Chem. Eng. Data* **1963**, *8*, 22–25.
[6] W. Engel, K. Menke, Development of propellants containing ammonium nitrate, *Def. Sci. J.* **1996**, *46*, 311–318.
[7] C. Oommen, S. R. Jain, Phase modification of ammonium nitrate by potassium salts, *J. Therm. Anal. Calorim.* **1999**, *55*, 903–918.
[8] A. N. Campbell, A. J. R. Campbell, The effect of a foreign substance on the transition: NH_4NO_3 IV $\leftrightarrow$ NH_4NO_3 III, *Can. J. Res.* **1946**, 24b, 93–108.
[9] P. J. Barrett, The shape of rock particles, a critical review, *Sedimentology* **1980**, *27*, 291–303.

Received: September 21, 2017
Revised: December 1, 2017
Published online: January 30, 2018

